AJNR

Apparent Diffusion Coefficients of Metabolites in Patients with MELAS Using Diffusion-Weighted MR Spectroscopy

Z. Liu, D. Zheng, X. Wang, J. Zhang, S. Xie, J. Xiao and X. Jiang

AJNR Am J Neuroradiol 2011, 32 (5) 898-902
doi: https://doi.org/10.3174/ajnr.A2395
http://www.ajnr.org/content/32/5/898

ORIGINAL RESEARCH

Apparent Diffusion Coefficients of Metabolites in Patients with MELAS Using Diffusion-Weighted MR Spectroscopy

Z. Liu
D. Zheng
X. Wang
J. Zhang
S. Xie
J. Xiao
X. Jiang

BACKGROUND AND PURPOSE: DW-MR spectroscopy can detect the diffusion coefficients of NAA, Cr, PCr, and Cho and can, therefore, provide some useful information. The aims of this study were to probe the mechanisms underlying the pathogenesis of MELAS and to see whether DW-MR spectroscopy is a useful technique for other diseases besides cerebral infarction.

MATERIALS AND METHODS: Fifteen healthy volunteers and 10 patients with MELAS were enrolled in the study. All were scanned on a 3T whole-body MR imaging scanner. Fifteen ADCs of the singlet metabolites in the gray matter of the healthy subjects, 10 ADCs of the singlet metabolites in the lesions, and 8 ADCs of the singlet metabolites in the nonaffected areas were used in the statistical analysis, respectively.

RESULTS: The metabolite ADCs of the nonaffected areas and the lesions in the patients were higher than those of the frontal gray matter in the healthy controls. There were significant differences between the metabolite ADCs of the nonaffected areas in patients and those in the healthy controls, and it was the same with the metabolite ADCs of the lesions and those of the healthy controls.

CONCLUSIONS: The increased ADC values of the metabolites reveal that MELAS is a mitochondrial neuronopathy and involves the entire brain. DW-MR spectroscopy is a very useful noninvasive technique, which can show some valuable information that conventional MR imaging cannot display. Thus, it can be applied to brain diseases besides cerebral infarction.

ABBREVIATIONS: ADC = apparent diffusion coefficient; ATP = adenosine triphosphate; Cho = choline; Cr = creatine; DW = diffusion-weighted; DWI = diffusion-weighted imaging; FLAIR = fluid-attenuated inversion recovery; MELAS = mitochondrial myopathy, encephalopathy, lactic acidosis, and stroke-like episodes; NAA = *N*-acetylaspartate; PCr = phosphocreatine; VOI = volume of interest

DWI can assess the diffusion of water molecules by applying the Stejskal-Tanner equation for calculating ADC value.[1] DWI has become an indispensable tool for the early detection of acute cerebral ischemia and assists in the diagnosis of other brain diseases, including neoplasms, infections, and traumatic injury.[2-5] Because water molecules can diffuse freely and exchange between both extracellular and intracellular compartments, the water ADC values reflect a weighted mean of the contributions from both.[6] Therefore, DWI cannot distinguish the extracellular water diffusion coefficients from the intracellular ones.[6,7]

DW-MR spectroscopy can detect the diffusion of intracellular metabolites, NAA, Cr, PCr, and Cho, which are exclusively located in the intracellular space and exchange very slowly between the 2 compartments.[8,9] Therefore, the detected metabolite ADCs are only attributed to diffusion in the intracellular space. However, due to the inherently low signal intensity–to-noise ratio, poor spatial resolution, pulse sequence unavailability, long scanning time, and limited brain coverage, DW-MR spectroscopy has not been widely used. As a result, there are few published studies and these focus mainly on healthy volunteers and patients with acute cerebral infarction.[10-16] According to the published research, the ADCs of NAA, Cr, and Cho reduce significantly in the acute phase of cerebral ischemia.[11,14-16] These studies have indicated that DW-MR spectroscopy is a useful noninvasive technique in detecting pathologic changes in the intracellular environment.

MELAS syndrome is one of the most common multisystem mitochondrial disorders, mainly affecting both the skeletal muscle and the central nervous system. It is characterized by a disorder in mitochondrial function due to point mutations of mitochondrial DNA, which impair ATP production.[17,18] However, until now, the exact mechanism of MELAS has not been fully elucidated. There are 2 basic hypotheses: ischemic and metabolic.[19] One theory is that the increased number of enlarged mitochondria in the vascular endothelial cells obstructs small cerebral arteries, leading to ischemic change.[20,21] The other hypothesis is that neuronal hyperexcitability increases energy demand and brings about energy imbalance in particularly susceptible neurons, which induces neuronal en-

Received August 16, 2010; accepted after revision September 18.

From the Department of Radiology (Z.L., X.W., S.X., J.X., X.J.), Center for Functional Imaging, Peking University First Hospital, Peking University, Beijing, China; Academy for Advanced Interdisciplinary Studies (D.Z.), Peking University, Beijing, China; and Academy for Advanced Interdisciplinary Studies and Department of College Engienering (J.Z.), Peking University, Beijing, China.

Z.L. and D.Z. contributed equally to this work.

This research was supported by the Fundamental Research Funds for the Central Universities, Ministry of Education of the People's Republic of China.

Please address correspondence to Xiaoying Wang, MD, Peking University First Hospital, Department of Radiology, 8 Xishiku St, Xicheng District, Bejing, 100034 China; e-mail: wangxy1@yahoo.com.cn and Jue Zhang, PhD, Department of Academy for Advanced Interdisciplinary Studies, Peking University, No. 5 Yiheyuan Rd, Haidian District, Beijing 100871, China; e-mail: zhangjue@pku.edu.cn

DOI 10.3174/ajnr.A2395

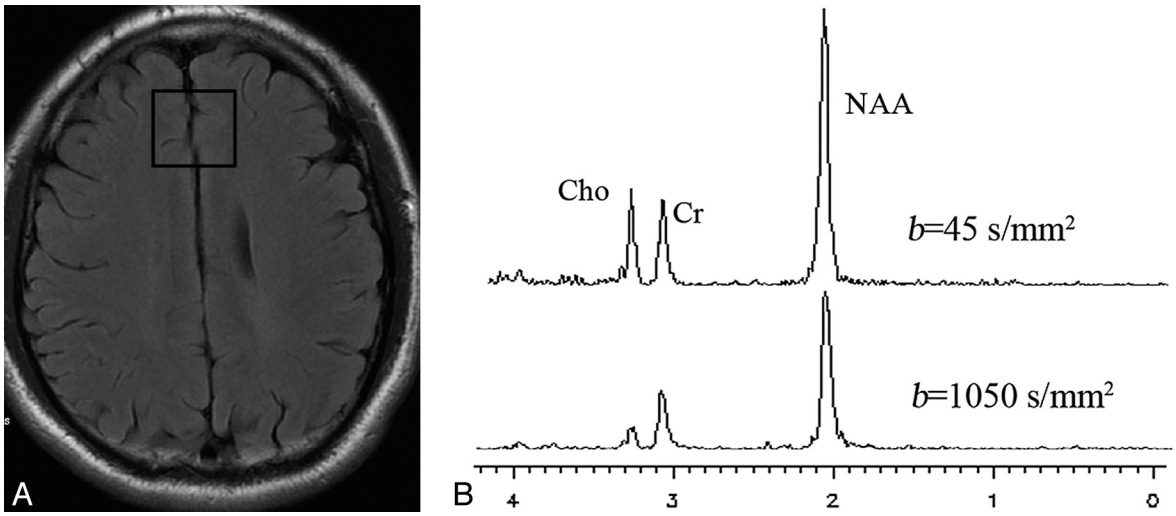

Fig 1. *A,* A VOI is seen in the gray matter of the frontal lobe in a healthy subject. *B,* MR spectroscopy was performed with a set of b-values (b=45 s/mm^2 and b=1050 s/mm^2).

ergy failure and necrosis.[17,22] Therefore, we applied DW-MR spectroscopy to probe the mechanisms underlying the pathogenesis of MELAS and to see whether it is a useful technique for other diseases besides ischemia.

Materials and Methods

Patients and Controls

This study was approved by our institutional review board. We used an 8-channel head coil to receive the signal intensity. The heads of the volunteers and patients were secured by using a vacuum pillow to hold them steady.

Ten patients with MELAS (6 males, 4 females; 12–43 years of age; mean age, 25 years) were enrolled. The diagnosis of MELAS syndrome was based on the clinical symptoms (seizures, dementia, and recurrent headache) and the finding of a mutation at the nucleotide position 3243 in the mitochondrial DNA by blood examination. All patients were in the interictal phase of MELAS.

Fifteen healthy patients without MELAS (9 males and 6 females; 15–41 years of age; mean age, 25 years) were enrolled to constitute an ideal age- and sex-matched population in the study. The criteria of the healthy control group were as follows: First, only healthy people without a history of headache, epilepsy, head trauma, hypertension, diabetes mellitus, or other significant medical conditions were selected. Second, those healthy subjects had normal findings on physical, neurologic, and mental state examinations and on brain MR images.

Pulse Sequence

The pulse sequence was implemented on a 3T whole-body MR imaging scanner (Signa HD; GE Healthcare, Milwaukee, Wisconsin). The gradient system in this scanner allows a maximum gradient strength of 40 mT/m and a slew rate of 150 T/m/s. The DW-MR spectroscopy sequence was based on a point-resolved proton spectroscopy composite technique[23] using the ideas proposed by Ellegood et al[12] and van der Toorn et al.[24] There was a 90° sinc pulse for excitation and 2 optimized 180° sinc pulses for refocusing. Every 2 pairs of diffusion-weighting gradients were present around both 180° pulses in 3 directions simultaneously.[24] Diffusion-weighting gradients were followed by crusher gradients in the x- and y-directions. Before excitation radio-frequency, there was a chemical shift selective suppression radio-frequency pulse sequence.[25]

In brief, 2 MR spectroscopy sequences with different b-values were compiled into a pulse sequence (DW-MR spectroscopy sequence). Therefore, a set of DW-MR spectroscopy series was obtained by a combination of 2 proton MR spectroscopy sequences localized to the same volume of interest. The first proton MR spectroscopy sequence had a b-value of 45 s/mm^2, and the second had a b-value of 1050 s/mm^2.

Postprocessing was conducted in the scanner by using Sage software (GE Healthcare), which consists of apodization with a Gaussian function, zero-filling, Fourier transformation, and zero-order phase correction. The spectra included an NAA peak (2.01 ppm), Cr and PCr peaks (3.0 ppm), and Cho-containing compound peaks (3.22 ppm). Peaks were fitted with a nonlinear least-squares fitting method assuming a Lorentzian line shape. A semilogarithmic plot of the peak heights against the b-values was fitted into the equation to obtain the ADC value.[10,13,24]

The ADC was calculated by using the following equation:

$$ADC = -\ln[S(b_2) / S(b_1)] / (b_2 - b_1),$$

where $S(b_1)$ and $S(b_2)$ are the signal intensities of the metabolites for the 2 MR spectroscopy sequences with different b-values, b_1, and b_2, and b is the factor of diffusion gradients.

MR Imaging Protocol

The MR imaging acquisition protocol included axial T2 FLAIR, T1 FLAIR, and DW-MR spectroscopy. The T2 FLAIR parameters were as follows: TR, 9600 ms; TE, 117 ms; and TI, 2400 ms. The T1 FLAIR parameters were the following: TR, 2300 ms; TE, 10 ms, and TI 960 ms. We used axial single-shot spin-echo echo-planar sequences to acquire DWI with the following parameters: TR/TE, 4000/70 ms; b=0; and 1000 s/mm^2.

DW-MR spectroscopy parameters were the following: TR, 2000 ms; TE, 144 ms; NEX, 16; spectral width, 5000 Hz; and data points, 4096. In all cases, selected volume size was 2 × 2 × 2 cm^3. B-values were 45 s/mm^2 and 1050 s/mm^2 in healthy subjects and in the patients with MELAS, respectively. Global shimming was performed with a standard nonselective shimming sequence. Then local shimming within the selected voxel was required to obtain a full width at half maximum of 2–5 Hz. The duration of a set of DW-MR spectroscopy series was 8 minutes 28 seconds.

The VOI was chosen in the following regions: the abnormal-in-

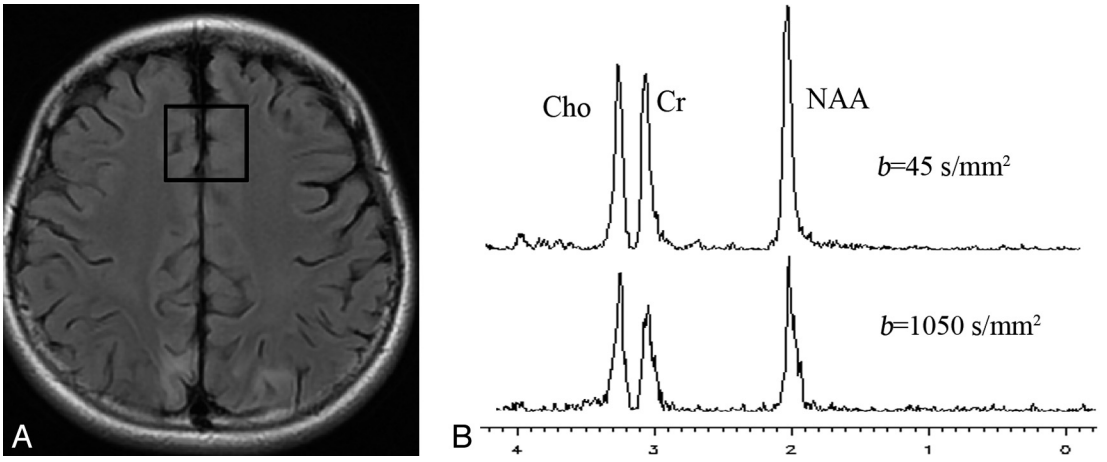

Fig 2. *A,* A VOI is seen in the nonaffected frontal lobe in a patient with MELAS. *B,* MR spectroscopy was performed with a set of b-values (b=45 s/mm^2 and b=1050 s/mm^2).

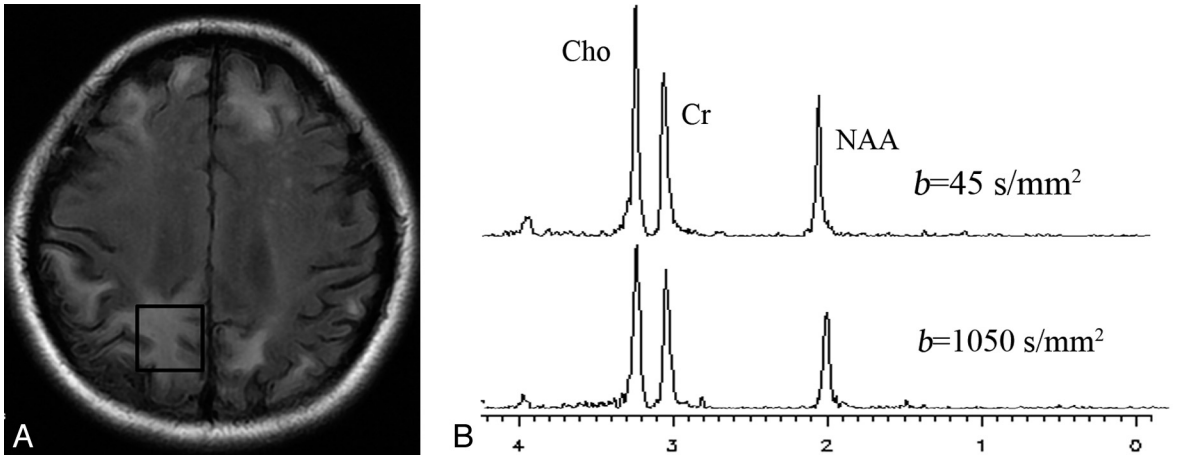

Fig 3. *A,* A VOI is seen in the previously affected area of the patient with MELAS. *B,* MR spectroscopy was performed with a set of b-values (b=45 s/mm^2 and b=1050 s/mm^2).

tensity areas in the DWI or T2 FLAIR or T1 FLAIR images, the nonaffected frontal gray matter of the patients, and the frontal gray matter of healthy subjects. The nonaffected areas were referred to as the normal-appearing areas in all the above-mentioned conventional MR images. A VOI of a healthy volunteer and a set of sample spectra are shown in Fig 1. The VOI in the nonaffected areas and the lesions of the patients and the corresponding spectra are illustrated in Figs 2 and 3, respectively.

Fifteen ADCs of the singlet metabolites in the frontal gray matter of the healthy subjects, 10 ADCs of the singlet metabolites in the lesions, and 8 ADCs of the singlet metabolites in the normal-appearing frontal gray matter were used in the statistical analysis, respectively.

Results

In the nonaffected frontal gray matter of the patients with MELAS, the ADCs of Cho, Cr, and NAA increased 50%, 50%, and 67%, respectively, and statistically significant differences ($P < .05$) were presented by the independent samples t test, relative to controls (Table 1).

Table 2 lists the ADCs of NAA, Cr, and Cho in the gray matter of healthy controls and in the lesions of the patients with MELAS. Compared with healthy controls, the ADC increases in the lesions were 35% for Cho, 55% for Cr, and 38% for NAA, and statistically significant differences ($P < .05$) were revealed by the independent samples t test (Table 2).

Table 1: ADC values (mean) of metabolites in the gray matter of healthy subjects and in nonaffected areas of patients with MELAS

Values ($\times 10^{-3}$mm^2/s)	Healthy Subjects (n = 15)	Nonaffected Areas in Patients (n = 8)	P Value
Cho	0.20 ± 0.07	0.30 ± 0.08	.00002
Cr	0.20 ± 0.07	0.30 ± 0.05	.00002
NAA	0.21 ± 0.05	0.35 ± 0.06	.00001

Table 2: ADCs (mean) of metabolites in the gray matter of healthy subjects and in lesions of patients with MELAS

Values ($\times 10^{-3}$mm^2/s)	Healthy Subject (n = 15)	Lesions in Patients with MELAS (n = 10)	P Value
Cho	0.20 ± 0.07	0.27 ± 0.07	.0002
Cr	0.20 ± 0.07	0.31 ± 0.11	.0002
NAA	0.21 ± 0.05	0.29 ± 0.06	.0001

Discussion

The results show that the metabolite ADCs of the healthy controls lie well within the range of the reported data and that there are only fine differences between ours and the published data in the healthy subjects.[10-13] The fine differences are attributed to the different diffusion times used in the DW-MR spectroscopy. Longer diffusion times can cause smaller ADC values for a given b-value in the restricted environment.[26,27]

NAA is primarily located in neurons.[28] Synthesis of NAA takes place in neuronal mitochondria via an ATP-related mechanism.[29,30] Then NAA is carried into the cytoplasm through active transport. Both Cho and Cr are mainly located in the cytosol.[31] In fact, the Cr-PCr system acts as a buffer for ATP homeostasis, and Cr increases in hypometabolic states and decreases in hypermetabolic states.[32,33]

In all cases in this study, the lactate peak was not present on MR spectroscopy. Because all these patients were in the interictal phase of MELAS, the quantity of lactate yielded by the brain cell was small; consequently, it was not detected by MR spectroscopy.

The major finding of this study is the ADC increases of 50%, 50%, and 67% for Cho, Cr, and NAA in the normal-appearing frontal gray matter of the patients with MELAS, compared with the healthy controls. There are some reasons for this result. First, brain cell swelling occurs during epilepsies or ischemia, both of which are 2 basic incentives for MELAS.[34] Neurons or astrocytes need to consume excess energy to maintain ion homeostasis and membrane stabilization. Because mitochondria play a central role in producing ATP and because the ATP-generating capacity is low in neurons and astrocytes in patients with MELAS,[35] mitochondrial defects can disturb ion homeostasis and destabilize brain cell membranes.[36] As a result, ions accumulate in the cells; thus, water molecules enter the cells, which expand their volume and dilute the viscosity and decrease the tortuosity in the cytoplasm.[37] Thus, ADCs of the metabolites in the nonaffected areas increase.

Second, due to the impaired oxidative phosphorylation, there may be disruption of the intracellular organelles. Under normal circumstances, these can restrict the diffusion of the metabolites. As a consequence, the ADC of the metabolites may rise. Third, because ATP generated in the mitochondria cannot satisfy the requirements for the synthesis and active transport of NAA,[38,39] it cannot pass through the mitochondrial membrane and stays in the mitochondria. At the ultrastructural level, most mitochondria in the nonaffected neurons are enlarged.[40] Therefore, the increase in the ADC of NAA is most pronounced among metabolites. Because the Cho concentration in astrocytes is twice that of neurons,[9] the increased ADC of Cho manifests that the astrocytes may also be involved in the pathology. This result is consistent with the conclusion that there is widespread cellular dysfunction in MELAS, not confined to either neuronal or vascular derangement.[41]

Compared with healthy controls, the ADC increases in the lesions were 35% for Cho, 55% for Cr, and 38% for NAA as seen in Table 2. Because the old ischemia-like lesions of MELAS are characterized by laminar necrosis and extensive neuronal loss,[42-44] some of the metabolites can leak into the extracellular space and the neuronal loss can lead to the expansion of the extracellular space, which augments the ADCs of the metabolites. As discussed above, there also may be disruption of intracellular organelles, which can increase the ADCs of the metabolites. Another reason is that much degenerative nuclear pyknosis in neurons is present in the cerebral cortex.[41] The pyknotic nuclei are far smaller than the normal nuclei.[45] Therefore, nuclear pyknosis can enlarge the intracellular space and consequently increase the ADCs of the metabolites. Furthermore, because the ATP cannot meet the energy needs, PCr is hydrolyzed to Cr to supply energy, which can increase the Cr ADC.[46] There is little or no ATP generated in the cells in the lesions, so the PCr barely exists in the cells, and only Cr contributes to the peak at 3.02. On the other hand, there may be PCr in the cells in the normal-appearing areas. Therefore, the Cr ADC of the lesions increases more than in the other areas and is higher than that of the normal-appearing areas.

There are some limits to this study. First, there was no brain pathology in the patients with MELAS. If there was pathology, we could compare the ADC of the metabolites with the pathologic change and, consequently, could draw a more exact conclusion. Second, we do not know the serial metabolite ADCs of the patients.

Conclusions

DW-MR spectroscopy shows that there is an increase in the metabolite ADCs of the previously affected and the nonaffected areas in patients with MELAS, compared with those of healthy controls. Those results directly demonstrate that MELAS is a mitochondrial neuronopathy and involves the entire brain. Therefore, DW-MR spectroscopy can find some useful intracellular pathophysiologic information that conventional MR imaging cannot display. In conclusion, it is a very useful noninvasive technique for brain diseases apart from cerebral infarction.

Acknowledgments

We thank Qiuling Li, MS, and Xiaofang Wang, MS, for their advice in drafting the manuscript.

References

1. Stejskal EO, Tanner JE. **Spin diffusion measurements: spin echoes in the presence of a time dependent field gradient.** *J Chem Phys* 1965;42:288–92
2. Busza AL, Allen KL, King MD, et al. **Diffusion-weighted imaging studies of cerebral ischemia in gerbils: potential relevance to energy failure.** *Stroke* 1992;23:1602–12
3. Schaefer PW, Grant PE, Gonzalez RG. **Diffusion-weighted MR imaging of the brain.** *Radiology* 2000;217:331–45
4. Liu Z, Liu X, Hui L, et al. **The appearance of ADCs in the non-affected areas of the patients with MELAS**. *Neuroradiology* 2011;53:227–32
5. Neumann-Haefelin T, Wittsack HJ, Wenserski F, et al. **Diffusion- and perfusion-weighted MRI: the DWI/PWI mismatch region in acute stroke.** *Stroke* 1999;30:1591–97
6. Wick M, Nagatomo Y, Prielmeier F. **Alteration of intracellular metabolite diffusion in rat brain in vivo during ischemia and reperfusion.** *Stroke* 1995;26:1930–34
7. Szafer A, Zhong J, Anderson AW, et al. **Diffusion-weighted imaging in tissues: theoretical models.** *NMR Biomed* 1995;8:289–96
8. Gujar SK, Maheshwari S, Bjorkman-Burtscher I, et al. **Magnetic resonance spectroscopy.** *J Neuroophthalmol* 2005;25:217–26
9. Hajek M, Dezortova M. **Introduction to clinical in vivo MR spectroscopy.** *Eur J Radiol* 2008;67:185–93
10. Posse S, Cuenod CA, Le Bihan D. **Human brain: proton diffusion MR spectroscopy.** *Radiology* 1993;188:719–25
11. Harada M, Uno M, Hong F, et al. **Diffusion-weighted in vivo localized proton MR spectroscopy of human cerebral ischemia and tumor.** *NMR Biomed* 2002;15:69–74
12. Ellegood J, Hanstock CC, and Beaulieu C. **Trace apparent diffusion coefficients of metabolites in human brain using diffusion weighted magnetic resonance spectroscopy.** *Magn Reson Med* 2005;53:1025–32
13. Ellegood J, Hanstock CC, Beaulieu C. **Diffusion tensor spectroscopy (DTS) of human brain.** *Magn Reson Med* 2006;55:1–8
14. Merboldt KD, Horstermann D, Hanicke W, et al. **Molecular self-diffusion of intracellular metabolites in rat brain in vivo investigated by localized proton NMR diffusion spectroscopy.** *Magn Reson Med* 1993;29:125–29
15. Wick M, Nagatomo Y, Prielmeier F, et al. **Alteration of intracellular metabolite diffusion in rat brain in vivo during ischemia and reperfusion.** *Stroke* 1995;26:1930–33

16. Abe O, Okubo T, Hayashi N, et al. **Temporal changes of the apparent diffusion coefficients of water and metabolites in rats with hemispheric infarction: experimental study of transhemispheric diaschisis in the contralateral hemisphere at 7 Tesla.** *J Cereb Blood Flow Metab* 2000;20:726–35
17. DiMauro S, Schon EA. **Mitochondrial respiratory-chain diseases.** *N Engl J Med* 2003;348:2656–68
18. Hanna MG, Nelson IP, Morgan-Hughes JA, et al. **MELAS: a new disease-associated mitochondrial DNA mutation and evidence for further genetic heterogeneity.** *J Neurol Neurosurg Psychiatry* 1998;65:512–17
19. Iizuka T, Sakai F, Suzuki N, et al. **Neuronal hyperexcitability in stroke-like episodes of MELAS syndrome.** *Neurology* 2002;59:816–24
20. Ohama E, Ohara S, Ikuta F, et al. **Mitochondrial angiopathy in cerebral blood vessels of mitochondrial encephalomyopathy.** *Acta Neuropathol* 1987;74:226–33
21. Takahashi N, Shimada T, Murakami Y, et al. **Vascular involvement in a patient with mitochondrial myopathy, encephalopathy, lactic acidosis, and stroke-like episodes.** *Am J Med Sci* 2005;329:265–66
22. Oppenheim C, Galanaud D, Samson Y, et al. **Can diffusion weighted magnetic resonance imaging help differentiate stroke from stroke-like events in MELAS?** *J Neurol Neurosurg Psychiatry* 2000;69:248–50
23. Nicolay K, Braun KPJ, de Graaf RA, et al. **Diffusion NMR spectroscopy.** *NMR Biomed* 2001;14:94–111
24. van der Toorn A, Dijkhuizen RM, Tulleken CA, et al. **Diffusion of metabolites in normal and ischemic rat brain measured by localized 1H MRS.** *Magn Reson Med* 1996;36:914–22
25. Haase A, Frahm J, Hanicke W, et al. **1H NMR chemical shift selective (CHESS) imaging.** *Phys Med Biol* 1985;30:341–44
26. Dreher W, Busch E, Leibfritz D. **Changes in apparent diffusion coefficients of metabolites in rat brain after middle cerebral artery occlusion measured by proton magnetic resonance spectroscopy.** *Magn Reson Med* 2001;45:383–89
27. Assaf Y, Cohen Y. **In vivo and in vitro bi-exponential diffusion of N-acetyl aspartate (NAA) in rat brain: a potential structural probe?** *NMR Biomed* 1998;11:67–74
28. Moffett JR, Namboodiri MA, Cangro CB, et al. **Immunohistochemical localization of N-acetylaspartate in rat brain.** *Neuroreport* 1991;2:131–34
29. Patel TB, Clark JB. **Synthesis of N-acetyl-L-aspartate by rat brain mitochondria and its involvement in mitochondrial/cytosolic carbon transport.** *Biochem J* 1979;184:539–46
30. Arun P, Moffett JR, Namboodiri MA. **Evidence for mitochondrial and cytoplasmic N-acetylaspartate synthesis in SH-SY5Y neuroblastoma cells.** *Neurochem Int* 2009;55:219–25. Epub 2009 Mar 17
31. Boulanger Y, Labelle M, Khiat A. **Role of phospholipase A(2) on the variations of the choline signal intensity observed by 1H magnetic resonance spectroscopy in brain diseases.** *Brain Res Rev* 2000;33:380–89
32. Wyss M, Kaddurah-Daouk R. **Creatine and creatinine metabolism.** *Physiol Rev* 2000;80:1107–213
33. Castillo M, Kwock L, Mukherji SK. **Clinical applications of proton MR spectroscopy.** *AJNR Am J Neuroradiol* 1996;17:1–15
34. Pasantes-Morales H, Tuz K. **Volume changes in neurons: hyperexcitability and neuronal death.** *Contrib Nephrol* 2006;152:221–40
35. Lindroos MM, Borra RJ, Parkkola R, et al. **Cerebral oxygen and glucose metabolism in patients with mitochondrial m. 3243A4G mutation.** *Brain* 2009: 132(pt 12);3274–3284
36. Iizuka T, Sakai F, Ide T, et al. **Regional cerebral blood flow and cerebrovascular reactivity during chronic stage of stroke-like episodes in MELAS: implication of neurovascular cellular mechanism.** *J Neurol Sci* 2007;257:126–38
37. Yonemura K, Hasegawa Y, Kimura K, et al. **Diffusion-weighted MR imaging in a case of mitochondrial myopathy, encephalopathy, lactic acidosis, and strokelike episodes.** *AJNR Am J Neuroradiol* 2001;22:269–72
38. Castillo M, Kwock L, Green C. **MELAS syndrome: imaging and proton MR spectroscopic findings.** *AJNR Am J Neuroradiol* 1995;16:233–39
39. Ducreux D, Nasser G, Lacroix C, et al. **MR diffusion tensor imaging, fiber tracking, and single-voxel spectroscopy findings in an unusual MELAS case.** *AJNR Am J Neuroradiol* 2005;26:1840–44
40. Katayama Y, Maeda K, Iizuka T. **Accumulation of oxidative stress around the stroke-like lesions of MELAS patients.** *Mitochondrion* 2009;9:306–13. Epub 2009 Apr 23
41. Gilchrist JM, Sikirica M, Stopa E, et al. **Adult-onset MELAS evidence for involvement of neurons as well as cerebral vasculature in strokelike episodes.** *Stroke* 1996;27:1420–23
42. Betts J, Jaros E, Perry RH, et al. **Molecular neuropathology of MELAS: level of heteroplasmy in individual neurones and evidence of extensive vascular involvement.** *Neuropathol Appl Neurobiol* 2006;32:359–73
43. Tanahashi C, Nakayama A, Yoshida M, et al. **MELAS with the mitochondrial DNA 3243 point mutation: a neuropathological study.** *Acta Neuropathol* 2000;99:31–38
44. Mizukami K, Sasaki M, Suzuki T, et al. **Central nervous system changes in mitochondrial encephalomyopathy: light and electron microscopic study.** *Acta Neuropathol* 1992;83:449–52
45. Burgoyne LA. **The mechanisms of pyknosis: hypercondensation and death.** *Exp Cell Res* 1999;248:214–22
46. Liess C, Radda GK, Clarke K. **Metabolite and water apparent diffusion coefficients in the isolated rat heart: effects of ischemia.** *Magn Reson Med* 2000;44: 208–14